Flux Angle Mapping Coaxial Magnetic Gears for High Gear Ratios

Salek A. Khan
Dept. of Electrical & Computer Engineering
University of Texas at Dallas
Richardson, Texas, United States
salek@utdallas.edu

Matthew C. Gardner
Dept. of Electrical & Computer Engineering
University of Texas at Dallas
Richardson, Texas, United States
matthew.gardner@utdallas.edu

Godwin Duan
Dept. of Electrical & Computer Engineering
Princeton University
Princeton, New Jersey, United States
gd9138@princeton.edu

***Abstract*—Magnetic gears use noncontact operation to achieve the same function as mechanical gears but benefit from a variety of potential advantages due to their noncontact power transfer. This paper proposes a new topology of coaxial magnetic gear that utilizes flux angle mapping (FAM). The ferromagnetic pieces (FPs) in the FAM magnetic gear are designed to map flux from any given electromagnetic angle in the inner airgap to the same electromagnetic angle in the outer airgap. The gear ratio is derived based on this mapping function. Using finite element analysis (FEA), the performance of the new topology is investigated by changing the shape, size and number of FPs. Additionally, the performance of the new topology is compared against a conventional coaxial magnetic gear at high gear ratios (≥ 40:1). Based on the FEA results, the proposed FAM CMG can obtain higher gravimetric torque densities (GTDs) than the conventional gear at high gear ratios. For example, at a gear ratio of 80, the FAM gear achieves about 250% as much GTD as the conventional gear. The FAM gear can be designed with symmetry to balance the magnetic forces on each rotor; however, this comes at the cost of reduced gear ratio.**

Keywords—Ferromagnetic pieces, finite-element analysis (FEA), flux angle mapping, gear ratio, magnetic gear, permanent magnet, torque density.

I. Introduction

Mechanical gears have a wide array of applications; however, due to the inherent physical contact between teeth, they have a few disadvantages. The mechanical contact between teeth causes frictional losses and wear, reduces reliability, and increases maintenance requirements. Magnetic gears can perform the same function as traditional mechanical gears but use modulated magnetic fields, instead of meshing teeth, to transfer power. This noncontact operation yields potential advantages, such as higher reliability, increased efficiency, overload protection, and reduced acoustic noise. Due to these advantages, magnetic gears have been proposed for a wide range of applications, including electric vehicles [1], [2], wind turbines [3], [4], ocean wave energy harvesting [5], [6], and ship propulsion [7], [8]. Coaxial magnetic gears are composed of permanent magnets (PMs), ferromagnetic back irons, and ferromagnetic pieces (called modulators for the conventional coaxial topology). Fig. 1(a) shows the conventional radial flux coaxial magnetic gear (CRCMG). For the CRCMG, the number of modulators (Q_2) for optimal operation is determined by the Rotor 1 and Rotor 3 pole counts according to (1)

$$Q_2 = P_1 + P_3 \tag{1}$$

where P_1 and P_3 are the number of pole pairs on Rotors 1 and 3, respectively. As described in [9], [10], the modulators create a permeance function that modulates the flux densities produced by the PMs on each rotor, creating the gearing effect. The largest gear ratio (G) is obtained by fixing Rotor 3, which yields

$$G|_{\omega_3=0} = \frac{\omega_1}{\omega_2} = \frac{Q_2}{P_1} \tag{2}$$

where ω_1, ω_2, and ω_3 represent the angular speeds of Rotors 1, 2, and 3 respectively.

The gear ratio of CRCMGs is increased by increasing the ratio of the number of modulators (Q_2) and Rotor 3 pole pairs (P_3) to the number of pole pairs on Rotor 1 (P_1), as described by (1) and (2). As demonstrated in [11]-[13], an increase in gear ratio generally reduces the efficiency and torque density of the CRCMG, and most CRCMG prototypes have had gear ratios less than 12:1 [11]. This performance degradation occurs because, at high gear ratios, the pole pair difference is quite high. Thus, the Rotor 3 PMs become very tangentially narrow, while the Rotor 1 PMs are tangentially very wide, as in Fig. 1(a); the difference in pole arc degrades performance, as it is impossible to simultaneously optimize both sets of PMs. Additionally, the wide Rotor 1 pole arcs require thick back irons to contain the flux paths, increasing the weight of the magnetic gear.

Thus, another topology that has been proposed for high gear ratios is the cycloidal magnetic gear (CyMG) [14]-[19]. However, CyMGs have significant mechanical challenges resulting from nonconcentric motion and inherently unbalanced forces [14]-[16], [20], [21]. These challenges result in a large number of bearings and large forces on the bearings, which can degrade their lifetime and efficiency [14].

This paper proposes a novel operating principle for magnetic gears, flux angle mapping (FAM). An example FAM gear is shown in Fig. 1(b). FAM gears avoid the nonconcentric motion of CyMGs, greatly simplifying their mechanical design. After deriving the gear ratios for FAM gears, the paper parametrically compares FAM gears against CRCMGs using 2D finite element analysis (FEA).

II. Operating Principle

In the FAM topology, the ferromagnetic pieces (FPs) serve a different function than in the CRCMG. When using FAM, the FPs are slanted to transfer flux from an electromagnetic angle on

Rotor 1 to the same electromagnetic angle on Rotor 3. This can be seen by comparing how the flux moves between the rotors in Fig. 2 (with FPs) and Fig. 3 (without FPs). At no load, as in Fig. 1(b), this means that the radially inner side of each FP is adjacent to the same polarity PM as the radially outer side. Thus, the FPs do not all share the same shape, and the number of FPs is not directly related to P_1 and P_3.

Fig. 4 illustrates the radial flux density created in the outer air gap by the inner PMs with or without the FPs. Without the FPs there is only the P_1 harmonic, which is 20 in this case. (Its multiples have too high order to appear on the graph.) However, with the FPs, there is a significant P_3 (21, in this case) harmonic. Mathematically, the FPs can be described by defining a mapping function from an angle in the outer airgap ($\emptyset_O$) to an angle in the inner airgap ($\emptyset_I$), as described by

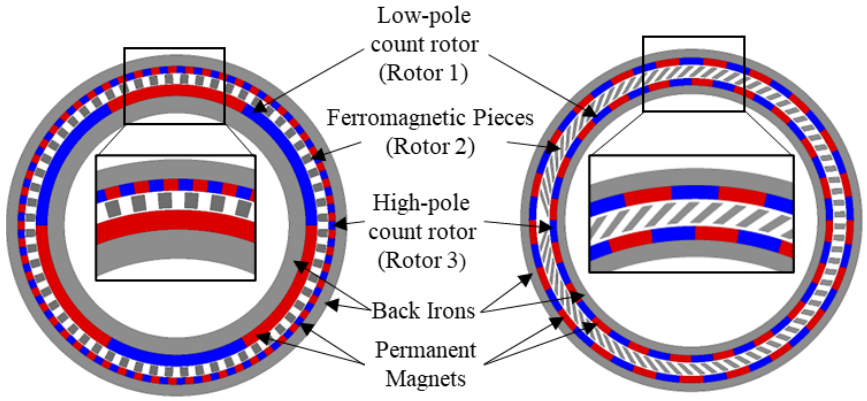

(a) (b)

Fig. 1: (a) The CRCMG topology and (b) the proposed FAM topology each with a gear ratio of 20:1.

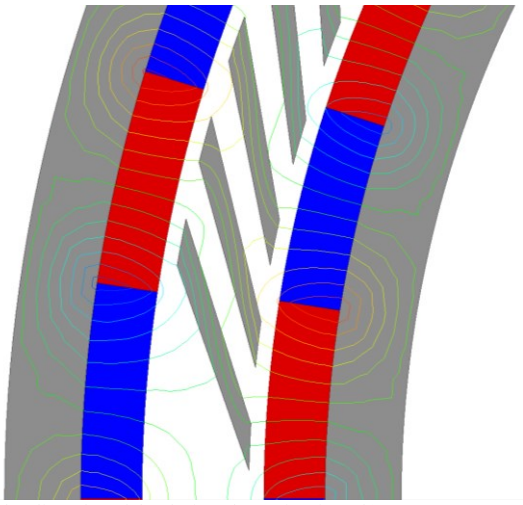

Fig. 2. Flux line plot of the design shown in Fig. 1(b)

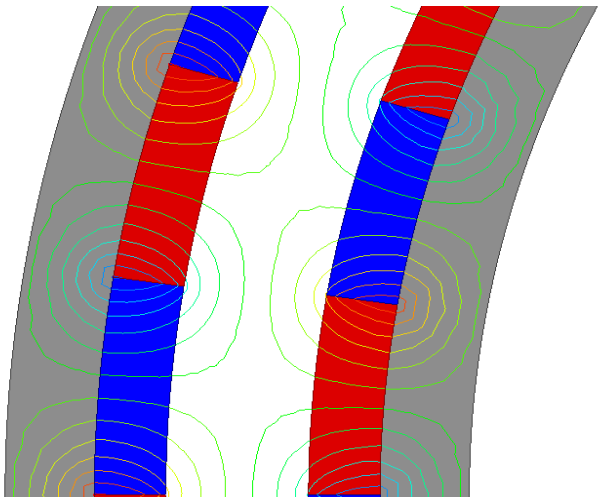

Fig. 3. Flux line plot of the design shown in Fig. 1(b) without FPs present

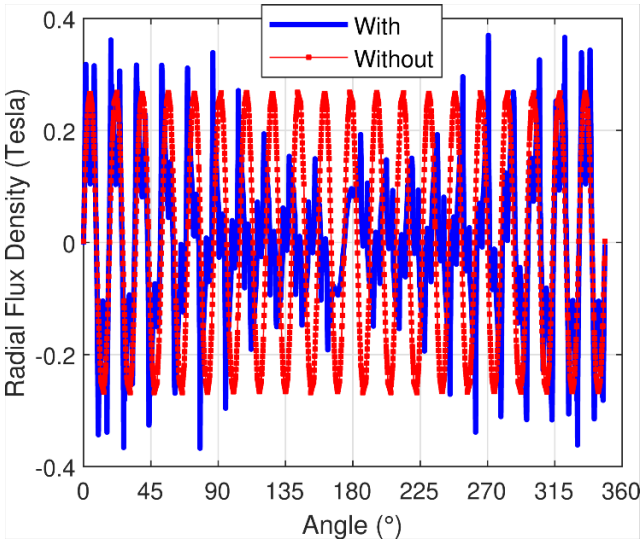

(a)

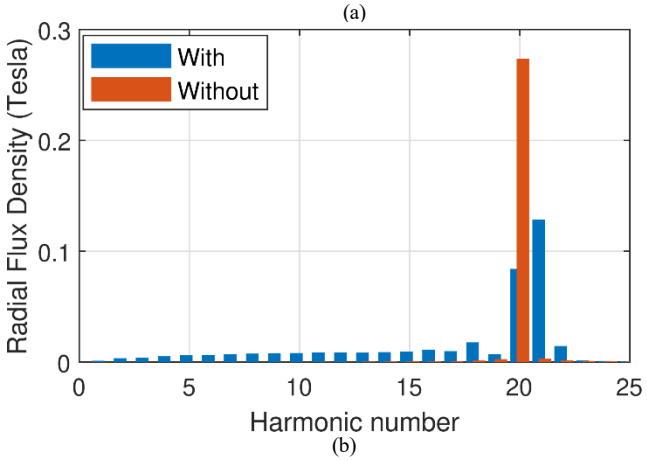

(b)

Fig. 4. (a) Radial flux density in the outer air gap generated by the Rotor 1 PMs with and without the FPs for the design in Fig. 1(b) and (b) the harmonic components.

$$\emptyset_I = \frac{P_3}{P_1}(\emptyset_O - \theta_2) + \theta_2, \quad (3)$$

where θ_2 is the angular position of the rotor holding the FPs (Rotor 2). The fundamental component of the MMF distribution in the inner airgap ($F_{PM1,In}$) produced by the Rotor 1 PMs can be described by

$$F_{PM1,In}(\emptyset_I) = F_1 \cos\big(P_1(\emptyset_I - \theta_1)\big), \quad (4)$$

where F_1 is the magnitude of the fundamental component and θ_1 is the angular position of Rotor 1. Applying the mapping function in (3) into the MMF equation in (4) yields the MMF distribution produced by the inner (Rotor 1) PMs in the outer airgap ($F_{PM1,Out}$) defined by

$$F_{PM1,Out}(\emptyset_O) = F_1 \cos(P_3\emptyset_O - (P_3 - P_1)\theta_2 - P_1\theta_1). \quad (5)$$

This yields an MMF distribution with P_3 pole pairs, which can interact with the outer (Rotor 3) PMs to produce torque. In steady-state, θ_2 and θ_1 can be expressed as functions of time (t) in terms of the Rotor 2 and Rotor 1 speeds (ω_2 and ω_1, respectively) and the Rotor 2 and Rotor 1 initial positions ($\theta_{2,0}$ and $\theta_{1,0}$, respectively), as given by

$$\theta_2 = \omega_2 t + \theta_{2,0} \quad (6)$$

$$\theta_1 = \omega_1 t + \theta_{1,0}. \quad (7)$$

If the outer (Rotor 3) PMs are stationary, the MMF distribution produced by the Rotor 1 PMs in the outer airgap should be stationary to interact with the stationary Rotor 3 PMs. Plugging (6) and (7) into (5) and keeping the MMF distribution stationary yields

$$-(P_3 - P_1)\omega_2 - P_1\omega_1 = 0, \quad (8)$$

which gives the gear ratio (G) given in

$$G|_{\omega_3=0} = \frac{\omega_2}{\omega_1} = \frac{-P_1}{P_3 - P_1}. \quad (9)$$

In (9) the negative sign indicates that the rotors rotate in opposite directions. From a practical perspective, it is likely reasonable for most applications to keep the outermost component (Rotor 3) stationary, yielding the gear ratio in (9). However, if Rotor 3 is rotating at a speed of ω_3, then the speed of the MMF distribution in (5) should rotate at the same electromagnetic speed as the Rotor 3 PMs. This yields

$$-(P_3 - P_1)\omega_2 - P_1\omega_1 = -P_3\omega_3, \quad (10)$$

which can be solved to produce the gear ratios resulting from keeping either Rotor 1 or Rotor 2 stationary:

$$G|_{\omega_1=0} = \frac{\omega_2}{\omega_3} = \frac{P_3}{P_3 - P_1} \quad (11)$$

$$G|_{\omega_2=0} = \frac{\omega_1}{\omega_3} = \frac{P_3}{P_1}. \quad (12)$$

If Rotor 1 is kept stationary, the gear ratio in (11) can be slightly higher than in (9), if Rotor 3 has more pole pairs than Rotor 1 due to its larger diameter. This comes at the disadvantage of having the outermost component rotating, but this may be acceptable or even desirable in some applications. On the other hand, keeping Rotor 2 stationary yields a low gear ratio, as in (12), unless a there is a large difference between P_1 and P_3. Such a large difference is undesirable because it would likely cause the design to perform poorly, as with the CRCMG at high gear ratios [11]-[13].

In the proposed FAM topology, according to (9), a high gear ratio can be achieved with a difference between P_1 and P_3 as small as one pole pair. This allows the PMs on Rotors 1 and 3 to have similar pole arcs, as in Fig. 1(a), potentially allowing for better performance at high gear ratios. Additionally, the FAM gears do not have such wide pole arcs, which avoids the need for thick and heavy back irons. Thus, we expect that FAM gears can outperform CRCMGs at high gear ratios.

III. Design Study

A design study with the parameter combinations shown in Table I was evaluated with 2D FEA for both the CRCMG and the FAM topologies. The PMs were assumed to be NdFeB N48SH at room temperature, and M19 was used for the ferromagnetic components. For the CRCMG, the Q_2 and P_3 values were selected to yield noninteger gear ratios near target gear ratios of 40, 60, and 80; this was done to reduce torque ripple as explained in [11]. Furthermore, the designs were simulated with radially magnetized PMs (Hb = 1) and with discrete Halbach arrays with tangentially magnetized PMs between the radially magnetized PMs (Hb = 2). Since

TABLE I. Simulated Parameters for the 2D FEA Design Study

Symbol and Description	Values		
	CRCMG	AFAM	SFAM
P_1-Number of pole pairs on rotor 1	3,4,5,6	40,60,80	80,120,160
Q_2 - Number of ferromagnetic pole pieces	$P_1 + P_3$	142,190…286	
P_3 - Number of pole pairs on rotor 3	118	41,61,81	82,122,162
R_{Out} - Outer radius (mm)	200		
T_{BI1} - Radial thickness of Rotor 1 back irons (mm)	0,5,10,20	0,5	
T_{PM1} - Radial thickness of Rotor 1 PMs	3,6…18		
T_{Fe} - Radial thickness of ferromagnetic pieces (mm)	4,8,12		
T_{BI3} - Radial thickness of Rotor 3 back irons (mm)	0,5		
T_{Gap} - Radial thickness of air gaps (mm)	1		
α_{Fe} - Angular fill factor of ferromagnetic pieces	0.4,0.45,0.5,0.6		
k_{PM} - PM thickness ratio	0.5,0.75,1		
Hb - Number of PM pieces per pole in Halbach array	1,2		

the number of FPs is not directly related to P_1 and P_3 for FAM designs, the difference in pole pair counts can be any positive integer. The case with $P_3 - P_1 = 1$, as shown in Fig. 1(b) is asymmetric, which may result in unbalanced magnetic forces. Thus, in addition to these asymmetric FAM (AFAM) cases, designs with $P_3 - P_1 = 2$ were also evaluated. Fig. 5 illustrates such a design with a gear ratio of 20:1. (Note that with a difference in pole counts larger than 1, the outer position of some FPs is shifted by a Rotor 3 pole pair pitch relative to the mapping function defined in (3) to reduce their length.) This yields symmetry, which can cancel out the unbalanced forces. However, these symmetric FAM (SFAM) cases require twice as many pole pairs on Rotors 1 and 3 to achieve the same gear ratio as the AFAM cases.

The PM thickness ratio, k_{PM}, was used to vary the radial thicknesses of the Rotor 3 PMs (T_{PM3}) based on the Rotor 1 PM radial thickness (T_{PM1}) as given by

$$k_{PM} = \frac{T_{PM3}}{T_{PM1}} \tag{13}$$

Two normalized metrics, volumetric torque density (VTD) and gravimetric torque density (GTD), are used to compare the topologies. The equations for these metrics are given by

$$VTD = \frac{Low\text{–}Speed\ Rotor\ Slip\ Torque}{Active\ Volume} \tag{14}$$

$$GTD = \frac{Low\text{–}Speed\ Rotor\ Slip\ Torque}{Active\ Mass} \tag{15}$$

The term “active volume” refers to the volume of the smallest cylinder enclosing all the active components, such as PMs, FPs, and rotor back irons, and does not include any housings, brackets, bearings, etc. Similarly, the term “active mass”, refers to the mass of the active components.

IV. Data Trends

Fig. 6 illustrates the torque densities defined in (14) and (15) for the CRCMG, AFAM and SFAM topologies. At gear ratios of about 60 and higher, the AFAM topology starts outperforming the CRCMG in terms of VTD. However, the SFAM topology consistently achieves lower VTD than both the CRCMG and AFAM topologies within the range of gear ratios evaluated. On the other hand, at least one of the FAM topologies achieves higher GTDs than the CRCMG across all gear ratios 40 and higher. For both VTD and GTD, the optimal SFAM design with a gear ratio of 40 ($P_1 = 80$, $P_3 = 82$) achieves approximately the same performance as the optimal AFAM design with a gear ratio of 80 ($P_1 = 80$, $P_3 = 81$), as these designs have very similar pole counts. For most cases within the range of high gear ratios evaluated, the AFAM outperforms the SFAM for a given gear ratio because the SFAM requires twice as many poles. However, because maximizing GTD tends to favor higher pole counts than maximizing VTD [22], the SFAM topology achieves higher GTDs than the AFAM topology at a gear ratio of 40. The

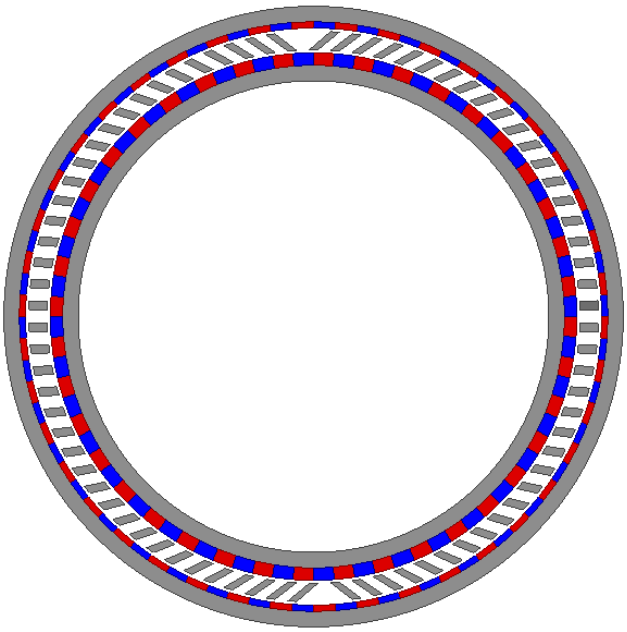

Fig. 5. An example of an SFAM design with a 20:1 gear ratio.

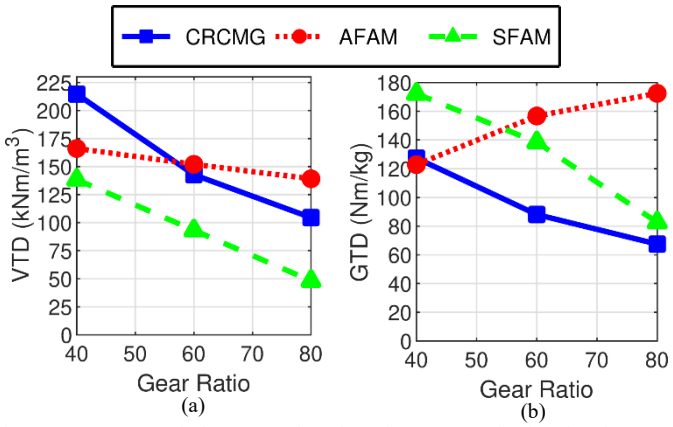

Fig. 6. (a) VTD and (b) GTD plotted against gear ratio for the three topologies.

benefits of FAM are more significant for GTD than VTD because the FAM topologies do not require very small Rotor 1 pole counts to achieve high gear ratios; these very low Rotor 1 pole counts tend to require thick back irons to contain the flux.

Fig. 7 shows the Rotor 1 forces for the maximum GTD designs in Fig. 6(b) with a stack length of 100 mm. Because of the symmetry present in the SFAM and CRCMG designs, they do not experience unbalanced magnetic forces [23]. However, the AFAM designs do experience significant unbalanced magnetic forces, which may require larger bearings and shafts and may increase bearing losses. Thus, in some cases, the SFAM topology may be preferable to the AFAM topology, even if the AFAM topology yields higher VTD or GTD based on only the magnetically active volume or mass.

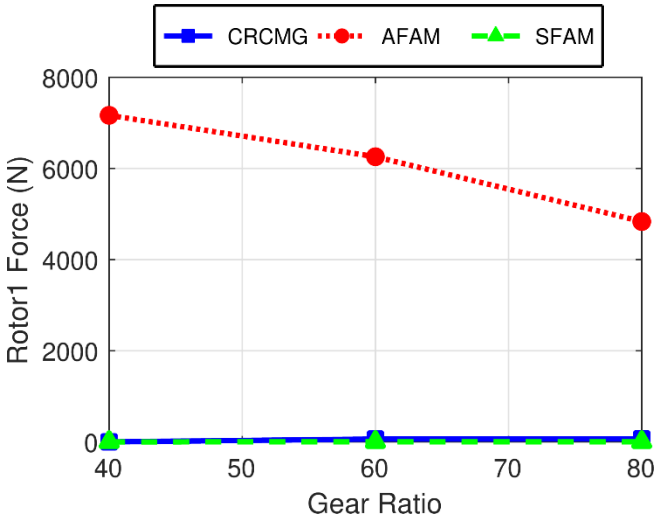

Fig. 7. The magnetic force on Rotor 1 for the maximum GTD designs in Fig. 6(b) with a stack length of 100 mm.

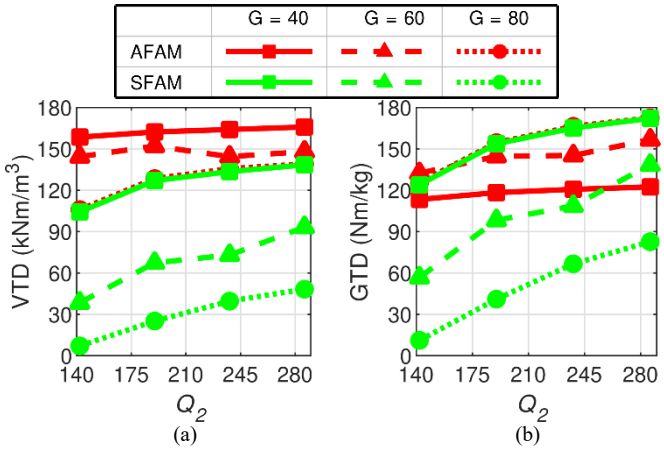

Fig. 8. (a) VTD and (b) GTD plotted against the number of FPs (Q_2) for the AFAM and SFAM topologies.

Fig. 8 shows how the number of FPs (Q_2) affects the VTD and GTD of the AFAM and SFAM topologies. Unlike the CRCMG, Q_2 is not directly related to P_1 and P_3 for the FAM topologies. Increasing Q_2 tends to increase both VTD and GTD, at least within the range of Q_2 values evaluated. Increasing Q_2 results in more FPs, each of which is tangentially thinner. While this may yield a slight increase in torque, it can also increase manufacturing complexity. As previously, the trends for AFAM designs with a gear ratio of 80 are almost identical to the trends for SFAM designs with a gear ratio of 40 because of the similarity in pole counts.

Fig. 9 shows how the radial thickness of the FPs (T_{Fe}) affects the VTD and GTD of the three topologies. In most cases, the designs prefer thinner FPs (within the range evaluated). However, the AFAM designs with the smallest gear ratio evaluated achieve maximum VTD and GTD with the intermediate FP radial thickness. All of the other cases have higher pole counts, particularly on Rotor 3, so the flux leakage between FPs causes the designs to favor radially thinner FPs.

Fig. 10 illustrates how the thickness of the PMs on Rotor 1 (T_{PM1}) affects the VTD and GTD of the three topologies. Generally, increasing the PM thickness is a means to cram more PM material into a design, which tends to increase VTD [22]. However, this also increases leakage flux, especially for designs with higher pole counts. Thus, thicker PMs provide more VTD benefits for the CRCMG designs, which have 3-6 Rotor 1 pole pairs, than for the AFAM designs, which have 40, 60, or 80 Rotor 1 pole pairs. For the higher gear ratio SFAM designs, which have up to 160 Rotor 1 pole pairs, increasing the PM thickness may even reduce VTD slightly. While increasing PM thickness does not affect the active volume (for a fixed outer radius and stack length), it does increase the active mass. Thicker magnets also increase the flux density and, consequently, may require thicker (and heavier) back irons to accommodate that flux. Thus, for each topology and gear ratio, the optimal PM thickness for maximizing GTD tends to be lower than the optimal PM thickness for maximizing VTD.

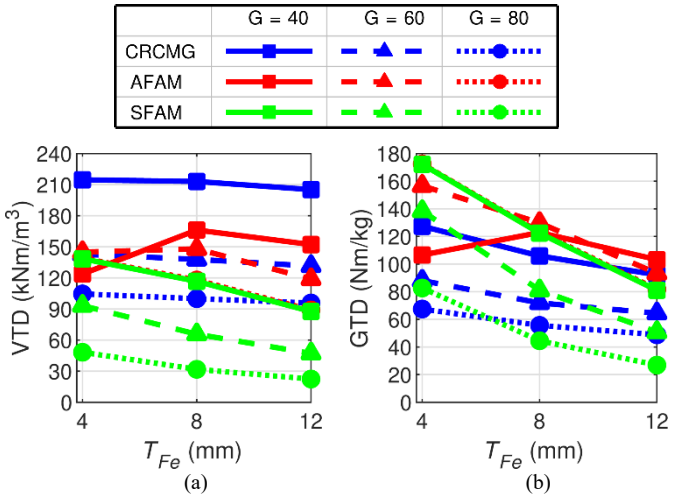

Fig. 9. (a) VTD and (b) GTD plotted against the thickness of the FPs (T_{Fe1}) for the three topologies.

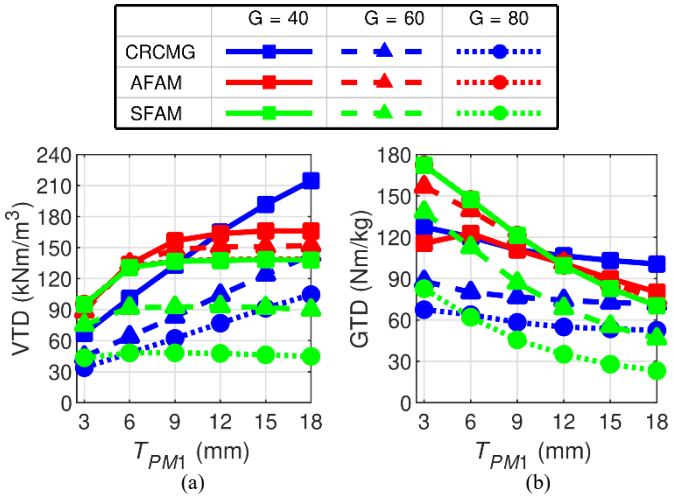

Fig. 10. (a) VTD and (b) GTD plotted against rotor 1 PM thickness (T_{PM1}) for the three topologies.

V. Conclusion

This paper introduces the FAM operating principle for magnetic gears and two new coaxial magnetic gear topologies (AFAM and SFAM) based on this principle. By utilizing FAM, the direct relationship between the number of FPs and the rotor pole counts is broken, allowing for better optimization at higher gear ratios. This independent relationship allows the difference in pole pairs in between Rotors 1 and 3 to be as small as one, which can allow a better matching of the pole counts at high gear ratios. However, the conventional coaxial magnetic gear requires a few large Rotor 1 poles and many tiny Rotor 3 poles in order to achieve a high gear ratio. The results of the FEA comparison between the FAM topologies and the CRCMG topology yield the following conclusions:

- AFAM gears can achieve higher VTDs than CRCMGs at very high gear ratios (at least 60 in this study). However, SFAM gears do not achieve as high VTDs.
- Both AFAM and SFAM gears can achieve higher GTDs than the CRCMG at high gear ratios.
- SFAM gears achieve their best performance at lower gear ratios than AFAM gears because SFAM gears require higher pole counts to achieve the same gear ratio.
- AFAM gears can experience significant unbalanced magnetic forces, but these are canceled by symmetry in the SFAM gears.
- Both AFAM and SFAM gears tend to benefit from increasing the number of FPs (within the range evaluated).
- However, each topology tends to prefer radially thinner FPs, except at the lowest pole count evaluated for AFAM.
- AFAM and SFAM gears see less torque increase from increasing the PM thickness than CRCMGs.

References

[1] T. V. Frandsen et al., “Motor integrated permanent magnet gear in a battery electrical vehicle,” *IEEE Trans. Ind. Appl.*, vol. 51, no. 2, pp. 1516-1525, Mar.-Apr. 2015.

[2] K. T. Chau, D. Zhang, J. Z. Jiang, C. Liu, and Y. Zhang, "Design of a Magnetic-Geared Outer-Rotor Permanent-Magnet Brushless Motor for Electric Vehicles," *IEEE Trans. Magn.*, vol. 43, no. 6, pp. 2504-2506, Jun. 2007.

[3] L. Jian, K. T. Chau, and J. Z. Jiang, “A magnetic-geared outer-rotor permanent-magnet brushless machine for wind power generation,” *IEEE Trans. Ind. Appl.*, vol. 45, no. 3, pp. 954–962, MayJun. 2009.

[4] K. Li, S. Modaresahmadi, W. B. Williams, J. Z. Bird, J. D. Wright, and D. Barnett, "Electromagnetic Analysis and Experimental Testing of a Flux Focusing Wind Turbine Magnetic Gearbox," *IEEE Trans. Energy Convers.*, vol. 34, no. 3, pp. 1512-1521, Sept. 2019.

[5] K. K. Uppalapati, J. Z. Bird, D. Jia, J. Garner, and A. Zhou, “Performance of a magnetic gear using ferrite magnets for low speed ocean power generation,” in *Proc. IEEE Energy Convers. Congr. Expo.*, 2012, pp. 3348– 3355.

[6] M. Johnson, M. C. Gardner, H. A. Toliyat, S. Englebretson, W. Ouyang, and C. Tschida, “Design, Construction, and Analysis of a Large Scale Inner Stator Radial Flux Magnetically Geared Generator for Wave Energy Conversion,” *IEEE. Trans. Ind. Appl.*, vol. 54, no. 4, pp. 3304 – 3314, Jul.-Aug. 2018.

[7] N. W. Frank, and H. A. Toliyat, “Gearing ratios of a magnetic gear for marine applications,” in *Proc. IEEE Elect. Ship Technol. Symp.*, 2009, pp. 477–481.

[8] H. Zhao, C. Liu, Z. Dong, R. Huang, and X. Li, "Design and Optimization of a Magnetic-Geared Direct-Drive Machine With V-Shaped Permanent Magnets for Ship Propulsion," *IEEE Trans. Transport. Electrific.*, vol. 8, no. 2, pp. 1619-1633, June 2022

[9] K. Atallah, and D. Howe, "A novel high-performance magnetic gear," *IEEE Trans. Magn.*, vol. 37, no. 4, pp. 2844-2846, July 2001.

[10] P. O. Rasmussen, T. O. Andersen, F. T. Jorgensen, and O. Nielsen, "Development of a high-performance magnetic gear," *IEEE Trans. Ind. Appl.*, vol. 41, no. 3, pp. 764-770, May-June 2005.

[11] B. Praslicka, M. C. Gardner, M. Johnson, and H. A. Toliyat, “Review and Analysis of Coaxial Magnetic Gear Pole Pair Count Selection Effects,” *IEEE Trans. Emerg. Sel. Topics Power Electron.*, vol. 10, no. 2, pp. 1813-1822, Apr. 2022.

[12] M. C. Gardner, B. Praslicka, M. Johnson, and H. A. Toliyat, "Optimization of Coaxial Magnetic Gear Design and Magnet Material Grade at Different Temperatures and Gear Ratios," *IEEE Trans. Energy Convers.*, vol. 36, no. 3, pp. 2493-2501, Sept. 2021.

[13] M. C. Gardner, M. Johnson, and H. A. Toliyat, “Analysis of High Gear Ratio Capabilities for Single-Stage, Series Multistage, and Compound Differential Coaxial Magnetic Gears,” *IEEE. Trans. Energy Convers.*, vol. 34, no. 2, pp. 665-672, Jun. 2019.

[14] B. Praslicka *et al*., “Practical Analysis and Design of a 50:1 Cycloidal Magnetic Gear with Balanced Off-Axis Moments and a High Specific Torque for Lunar Robots” in *Proc. IEEE Int. Elect. Mach. and Drives Conf.*, 2021, pp. 1-8.

[15] K. Davey, T. Hutson, L. McDonald, and G. Hutson, "The design and construction of cycloidal magnetic gears," in *Proc. IEEE Int. Elect. Mach. and Drives Conf.*, 2017, pp. 1-6.

[16] H. Huang, J. Z. Bird, A. L. Vera, and R. Qu, "An Axial Cycloidal Magnetic Gear That Minimizes the Unbalanced Radial Force," *IEEE Trans. Magn.*, vol. 56, no. 7, pp. 1-10, July 2020.

[17] F. T. Joergensen, T. O. Andersen, and P. O. Rasmussen, "The cycloid permanent magnetic gear," *IEEE Trans. Ind. Appl.*, vol. 44, no. 6, pp. 1659-1665, Nov.-Dec. 2008.

[18] J. Rens, K. Atallah, S. D. Calverley and D. Howe, "A Novel Magnetic Harmonic Gear," *IEEE Trans. Ind. Appl.*, vol. 46, no. 1, pp. 206-212, Jan.-Feb. 2010.

[19] M. C. Gardner, M. Johnson, and H. A. Toliyat, “Comparison of Surface Permanent Magnet Coaxial and Cycloidal Radial Flux Magnetic Gears,” in *Proc. IEEE Energy Convers. Congr. and Expo*, 2018, pp. 5005-5012.

[20] G. Duan *et al.*, “Cycloidal Magnetic Gear Combining Axial and Radial Topologies,” *IEEE Trans. Energy Convers*., early access.

[21] S. Hasanpour, M. Johnson, M. C. Gardner, and H. A. Toliyat, “Cycloidal Reluctance Magnetic Gears for High Gear Ratio Applications,” *IEEE Trans. Magn.*, early access.

[22] M. C. Gardner, B. E. Jack, M. Johnson, and H. A. Toliyat, “Comparison of Surface Mounted Permanent Magnet Coaxial Radial Flux Magnetic Gears Independently Optimized for Volume, Cost, and Mass,” *IEEE. Trans. Ind. Appl.*, vol. 54, no. 3, pp. 2237-2245, May-Jun. 2018.

[23] G. Jungmayr, J. Loeffler, B. Winter, F. Jeske, and W. Amrhein, "Magnetic Gear: Radial Force, Cogging Torque, Skewing, and Optimization," *IEEE. Trans. Ind. Appl*, vol. 52, no. 5, pp. 3822-3830, Sept.-Oct. 2016